



Computer simulation of electron energy levels for different shape InAs/GaAs semiconductor quantum dots

Yiming Li^{a,*}, O. Voskoboynikov^{a,b}, C.P. Lee^a, S.M. Sze^a

^a Department of Electronics Engineering, National Chiao Tung University, Hsinchu 300, Taiwan

^b Kiev Taras Shevchenko University, 252030 Kiev, Ukraine

Accepted 13 July 2001

Abstract

A computational technique for the energy levels calculation of an electron confined by a 3D InAs quantum dot (QD) embedded in GaAs semiconductor matrix is presented. Based on the effective one electronic band Hamiltonian, the energy and position dependent electron effective mass approximation, a finite height hard-wall 3D confinement potential, and the Ben Daniel–Duke boundary conditions, the problem is formulated and solved for the disk, ellipsoid, and conical-shaped InAs/GaAs QDs. To calculate the ground state and first excited state energy levels, the nonlinear 3D Schrödinger is solved with a developed nonlinear iterative algorithm to obtain the final self-consistent solutions. In the iteration loops, the Schrödinger equation is discretized with a nonuniform mesh finite difference method, and the corresponding matrix eigenvalue problem is solved with the balanced and shifted QR method. The proposed computational method has a monotonically convergent property for all simulation cases. The computed results show that for different quantum dot shapes, the parabolic band approximation is applicable only for relatively large dot volume. For the first excited states the non-parabolicity effect also has been found to be stronger than it at ground state. The QD model and numerical method presented here provide a novel way to calculate the energy levels of QD and it is also useful to clarify principal dependencies of QD energy states on material band parameter and QDs size for various QD shapes. © 2001 Elsevier Science B.V. All rights reserved.

PACS: 73.20.Dx; 73.61.-r; 03.65.Ge; 02.60.Cb

Keywords: InAs/GaAs; Semiconductor quantum dot; Dot shapes; Electron energy levels; Computer simulation

1. Introduction

In recent years, the study of semiconductor quantum dots (QDs) has been of a great interest (see [1–4] and references therein). Especially, during the last decade with modern nanotechnologies, it has become possible to fabricate realistic semiconductor QDs in laboratories. Unique electronic characteristics of the QDs

make it possible to model atomic physics in macroscopic systems experimentally and theoretically [5]. The semiconductor QDs are very attractive in micro- and nano-optoelectronics applications; furthermore, the spectral broadening in semiconductor quantum dots caused by the nonuniformity in the QD size and shape is the major concerns in the practical laser and optical applications [1,4,6–8]. Various experimental results demonstrate the InAs/GaAs quantum dots can have diverse shapes, such as disk, ellipsoid, or conical shapes with a circular top view cross section and

* Corresponding author.

E-mail address: ymli.ee87g@nctu.edu.tw (Y. Li).

a large area-to-height aspect ratio [9–15]. The shape of quantum dots is debated intensively in theoretical works, since an accurate calculation of the electronic structure obviously depends on the dot shape. The commonly used shapes include disk [16,17], ellipsoid [18,19], and conical shapes [20,21]. The energy level calculation has been done using the effective-mass approximation with [16,17,20–26] and without [18,19,27,28] the coordinate dependence for the effective mass. The variations in the dot size and shape can produce an energy fluctuation significantly in the strong confinement region. In addition, the theoretical modeling of quantum dot electronic properties can be done by different schemes. For a class of different models [16,20,24,27,29–33], one needs an assumption about the electronic confinement potential in the system. Among those used confinement poten-

tial models (the parabolic lateral potential, the infinite wall potential), a finite hard wall boundary potential model is the most realistic. However, in this case the nonlinear model problem cannot be solved analytically and exactly, and on the other hand the computer simulation provides a new alternative to solve the problem numerically. Unfortunately, most of developed calculation were done within only the simple parabolic band approximation for the electron effective mass [24,27,31–33]. It will produce an error in the electron energy level estimations for InAs/GaAs semiconductor QDs.

In this study we calculate and compare the electron energy spectra for three-dimensional small InAs/GaAs quantum dots of different shapes (see Fig. 1): disk, ellipsoid, and conical shape. All of them are cylindrically symmetric (with the circular top view cross

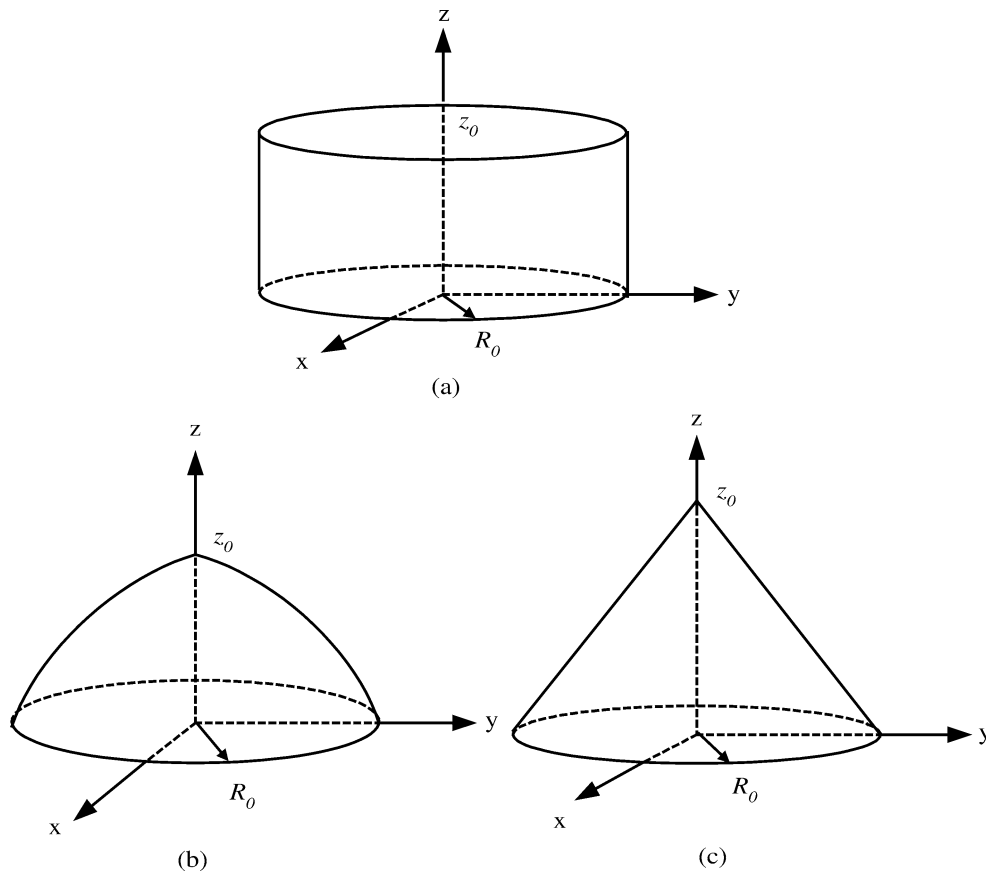


Fig. 1. Schematic diagrams for different shapes semiconductor QD: (a) disk-shaped, (b) ellipsoid-shaped, and (c) conical-shaped QD.

section). We use the effective one electronic band Hamiltonian, the energy and position dependent effective mass (non-parabolic) approximation, and the Ben Daniel–Duke boundary conditions in this study. A hard-wall (of finite height) 3D confinement potential induced by real discontinuity of the conduction band at the edge of the dot is also considered in the simulation. To calculate the ground state and first excited state energy levels, the nonlinear 3D Schrödinger is solved with a novel nonlinear iterative algorithm to obtain the final self-consistent solutions. The nonlinear iteration scheme consists of (i) set an initial energy E for starting simulation, (ii) compute effective mass $m(E, r)$ with the energy E , (iii) solve the Schrödinger equation for the energy E , (iv) update the newer energy and back to step (ii). The feedback iteration will be terminated when a specified stopping criterion on energy is reached. In the iteration loops, the Schrödinger equation is discretized with a nonuniform mesh finite difference method [34], and the corresponding matrix eigenvalue problem is solved with the balanced and shifted QR method [35]. The inverse iteration technique [36,37] is also applied to calculate the wave functions. The proposed computational method has a monotonically convergent property for all simulation cases. The computed results show that for different quantum dot shapes, the parabolic band approximation is applicable only for large dot volume. For the first excited states the non-parabolicity effect also has been found to be stronger than it at ground state.

This paper is organized as follows. In Section 2, the model and computer simulation algorithm are stated. The results and discussion are presented in Section 3. Section 4 is the conclusion.

2. Model and simulation technique

We consider semiconductor QDs in the one-band envelope-function formalism for electrons in which the effective Hamiltonian is given by [38,39]

$$\hat{H} = -\frac{\hbar^2}{2} \nabla_{\mathbf{r}} \left(\frac{1}{m(E, \mathbf{r})} \right) \nabla_{\mathbf{r}} + V(\mathbf{r}), \quad (1)$$

where $\nabla_{\mathbf{r}}$ stands for the spatial gradient, $m(E, \mathbf{r})$, the electron effective mass, is a function of both energy E and position. The expression of $m(E, \mathbf{r})$ is as follows:

$$\frac{1}{m(E, \mathbf{r})} = \frac{P^2}{\hbar^2} \left[\frac{2}{E + E_g(\mathbf{r}) - E_c(\mathbf{r})} + \frac{1}{E + E_g(\mathbf{r}) + \Delta(\mathbf{r}) - E_c(\mathbf{r})} \right], \quad (2)$$

$V(\mathbf{r}) = E_c(\mathbf{r})$ is the confinement potential, $E_c(\mathbf{r})$, $E_g(\mathbf{r})$ and $\Delta(\mathbf{r})$ denote, respectively, the position dependent electron band edge, band gap, and the spin-orbit splitting in the valence band, and P is the momentum matrix element.

We investigate quantum dots of disk, ellipsoid, and conical shapes with the base (top view) radius R_0 and height z_0 in the cylindrical coordinates (R, ϕ, z) . Since the system is cylindrically symmetric, the wave function can be written as

$$\Psi(\mathbf{r}) = \Phi(R, z) \exp(il\phi), \quad (3)$$

where $l = 0, \pm 1, \pm 2, \dots$ is the electron orbital quantum number. It remains to be a two-dimensional problem in (R, z) coordinates:

$$-\frac{\hbar^2}{2m_i(E)} \left(\frac{\partial^2}{\partial R^2} + \frac{\partial}{R\partial R} + \frac{\partial^2}{\partial z^2} - \frac{l^2}{R^2} \right) \Phi_i(R, z) + V_i(R, z) \Phi_i(R, z) = E \Phi_i(R, z), \quad (4)$$

where $V_1(R, z) = 0$ ($i = 1$) inside and $V_2(R, z) = V_0$ ($i = 2$) outside the dot. The boundary conditions are

$$\Phi_1(R, z) = \Phi_2(R, z), \quad z = f_S(R),$$

$$\frac{1}{m_1(E)} \left\{ \frac{\partial \Phi_1(R, z)}{\partial R} + \frac{df_S}{dR} \frac{\partial \Phi_1(R, z)}{\partial z} \right\} \Big|_{z=f_S(R)} = \frac{1}{m_2(E)} \left\{ \frac{\partial \Phi_2(R, z)}{\partial R} + \frac{df_S}{dR} \frac{\partial \Phi_2(R, z)}{\partial z} \right\} \Big|_{z=f_S(R)}, \quad (5)$$

where $z = f_S(R)$ (S is disk, ellipsoid, or conical-shaped QD) is the contour of the structure's cross section on the (R, z) plane. The structure shape is generated by the rotation of this contour around the z -axis.

Based on the fact that the electron effective mass is a spatial and energy dependent function, the Schrödinger equation is a nonlinear equation in energy. It is evident that the dependence relationship is not only appearing in Schrödinger equation itself but also on the boundary conditions of the model. To compute the final convergent solution of the model for different shape QDs self-consistently, a computational algorithm, as shown

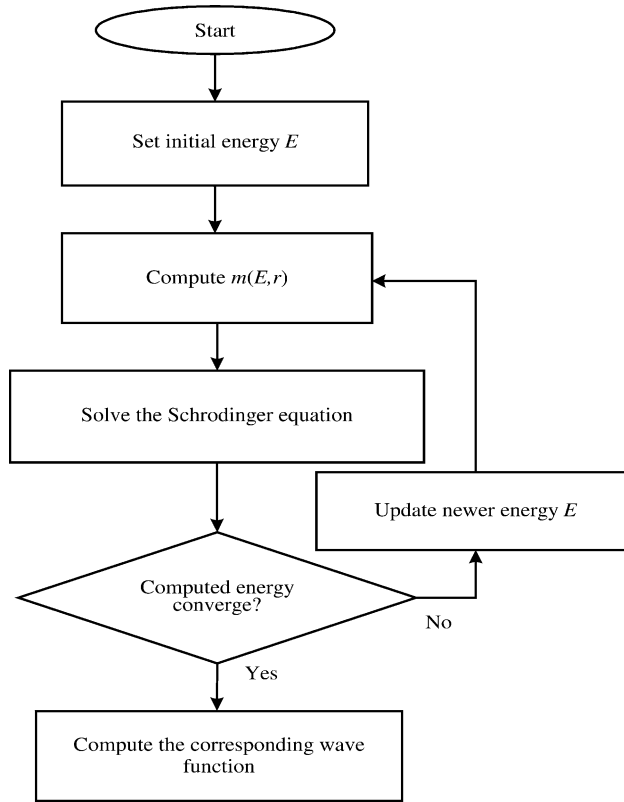


Fig. 2. A solution procedure for the semiconductor QD simulation.

in Fig. 2, for such nonlinear problem is proposed. Due to the energy dependence of the electron effective mass, our calculation consists of iteration loops to reach a “self-consistent” energy solution. The nonlinear iteration scheme consists of (i) set an initial energy E for starting simulation, (ii) compute effective mass $m(E, r)$ with the energy E , (iii) solve the Schrödinger equation for the energy E , (iv) update the newer energy and back to step (ii). The feedback iteration will be terminated when a specified stopping criterion on energy is reached. In each iteration we use a central difference method with nonuniform mesh technique [34] to discretize the nonlinear Schrödinger equation for disk, ellipsoid, and conical-shaped QDs. The discretized Schrödinger equation together with its boundary conditions (5) leads to a matrix eigenvalue problem

$$A\mathbf{X} = \lambda\mathbf{X}, \quad (6)$$

where A is the matrix rising from the discretized Schrödinger equation and boundary conditions, \mathbf{X} and λ are the corresponding eigenvectors (wave functions) and the eigenvalues (energy levels).

In the solution of this matrix eigenvalue problem, the QR algorithm is applied. The QR method is the dominant method for solving nonsymmetric matrix eigenvalue problem [35]. Because the matrix A in Eq. (6) is an energy dependent, five diagonal, nonsymmetric, and large sparse matrix, the eigenvalues of such matrix can be very sensitive to small changes in the matrix elements [40]. Therefore, a balancing algorithm to reduce the sensitivity of eigenvalues of the matrix A to small changes in the matrix elements is used firstly [36,40]. The main idea of balancing is making use of similarity transformations to set corresponding rows and columns of the matrix have comparable norms, thus reducing the overall norm of the matrix while leaving the eigenvalues unchanged. Then

the balanced matrix A is transformed into a simpler upper Hessenberg form [36,40]. In this transformation process, the elimination method is applied to reduce the balanced matrix A to the Hessenberg matrix form. The eigenvalues of the upper Hessenberg matrix are directly computed with the shifted QR method [35,36,40]. The balanced and shifted QR scheme used for the eigenvalues calculation is the most stable and robust method in semiconductor QD simulation. When an eigenvalue is found, the corresponding eigenvector of this eigenvalue is calculated with the inverse iteration method [36,37]. The fundamental idea of this method is to solve the linear system

$$(A - \zeta I)y = b, \quad (7)$$

where b is a trial vector and ζ is one of the computed eigenvalues of matrix A . The solution y will be the candidate for the eigenvector corresponding to ζ . In the solution of Eq. (7), we set the trial vector b to be a nonzero unit vector. The exact wave function should vanish only at infinity physically, but to simulate the QD within a finite region efficiently we have to set a zero value at a finite distance artificially. This computational consideration is designed only for the numerical simulation purpose. The artificial boundary is taken far enough so that it does not significant affect the results. In our calculation experience, the proposed

computational method converges monotonically and a strict convergence criteria (the maximum norm error is less than 10^{-15} eV) on energies can be reached by only 14–15 feedback nonlinear iterative loops.

3. Results and discussion

The energy spectrum of the dot consists of a set of discrete levels numerated by the set of numbers $\{n, l\}$, where n is the n th solution of the problem with the fixed l . In the calculations of the electron energy spectra for narrow gap InAs cylindrical QDs in GaAs matrix we choose the semiconductor band structure parameters [41] for InAs: energy gap is $E_{1g} = 0.42$ eV, spin-orbit splitting is $\Delta_1 = 0.48$ eV, the value of the non-parabolicity parameter is $E_{1p} = 3m_0P_1^2/\hbar^2 = 22.2$ eV, m_0 is the free electron effective mass. For GaAs we choose: $E_{2g} = 1.52$ eV, $\Delta_2 = 0.34$ eV, $E_{2p} = 24.2$ eV. The band offset is taken as $V_0 = 0.77$ eV. First of all, to test the robustness of the algorithm, we present the achieved convergence rate of the proposed nonlinear iterative algorithm. As shown in Fig. 3, this method compute energy efficiently and has a good convergent rate for the ground state energy level calculation with non-

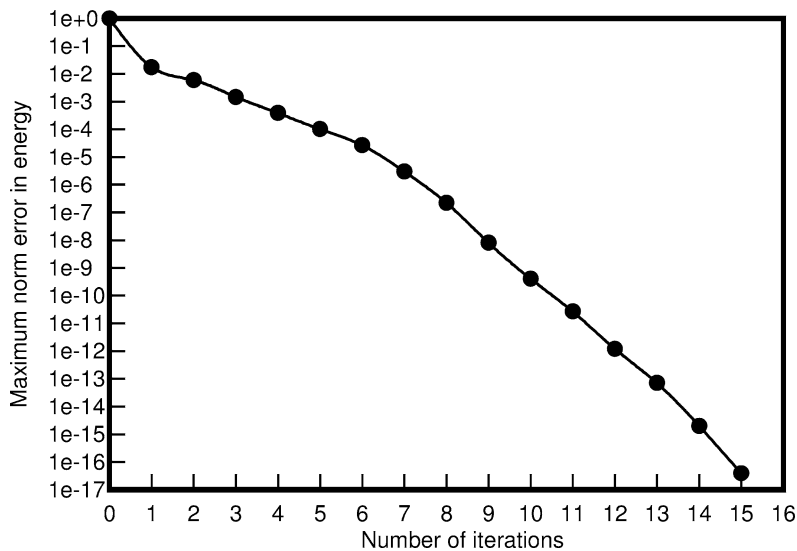


Fig. 3. The achieved convergent rate of the proposed iterative scheme for the ground state energy level calculation.

parabolic band approximation, where the dot shape is taken as conical-shaped QD, $R_0 = 10.0$ nm, the dot volume $V = 750 \text{ nm}^3$, and $(n = 1, l = 0)$. In addition, we also obtain similar convergent results for other simulation cases with various QD sizes and shapes.

As shown in Fig. 4, the calculated ground state $\{1,0\}$ energy depending on the dot volume is presented. For all calculations, the radius R is fixed at 10.0 nm. For a fixed dot volume V , the disk-shaped QD has higher geometry aspect ratio, so it has higher energy level for both the parabolic and non-parabolic band approximations than other shapes. For the first excited state, as shown in Fig. 5, we also have similar comparison results. Furthermore, the non-parabolic correction leads to a decreasing in the state energy

when dot volume is increased. The difference between parabolic (when $m_i(E) = m_{i0}$, $i = 1, 2$ — the band edge electronic effective mass) and non-parabolic approximation results gains ~ 0.15 eV for the disk-shaped QD with the dot volume $V \approx 750 \text{ nm}^3$. This difference can exceed known electron–electron interaction corrections [24,27,31–33]. For dots have large volume ($V > 2000 \text{ nm}^3$) the results from parabolic band approximation converge to the results calculated with non-parabolic band approximation. Fig. 5 shows the first $\{1,1\}$ excited energy states of the dot. As can be seen from the figure, the non-parabolic approximation leads to large corrections in this case. A difference in energy between parabolic and non-parabolic estimations can gain 0.2 eV for conical shape QD.

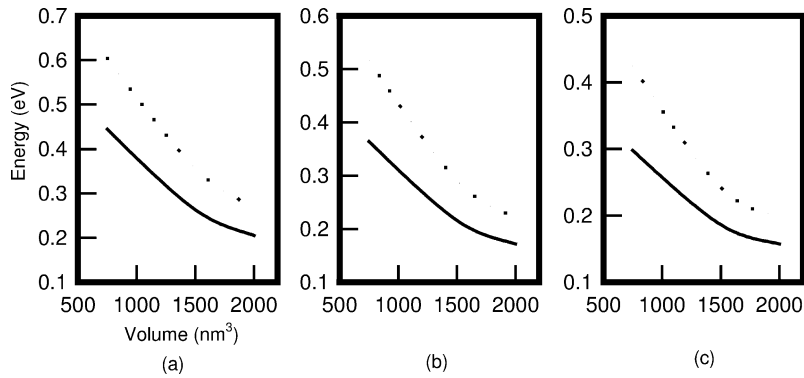


Fig. 4. Ground state ($l = 0$) energy with non-parabolic (solid line) and parabolic (dot line) band effective mass approximations for (a) disk, (b) ellipsoid, and (c) conical shape InAs/GaAs QDs.

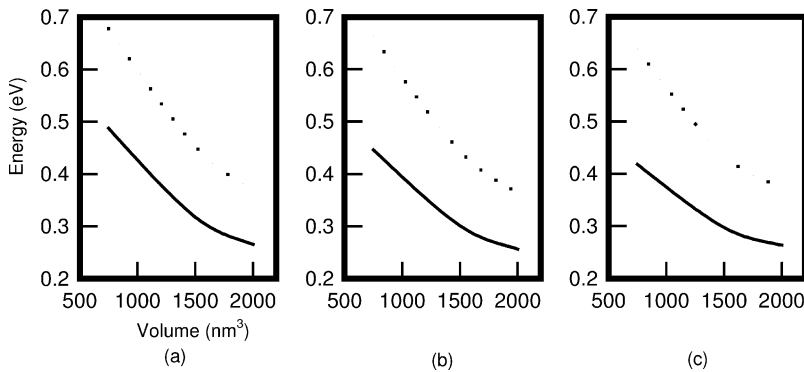


Fig. 5. Excited state ($l = 1$) energy with non-parabolic (solid line) and parabolic (dot line) band effective mass approximations for (a) disk, (b) ellipsoid, and (c) conical shape InAs/GaAs QDs.

4. Conclusion

A novel computational technique for the energy levels calculation of an electron confined by a 3D InAs quantum dot embedded in GaAs semiconductor matrix has been presented. With the developed QD simulator, we have found that the widely used the parabolic band approximation lead to a large discrepancy in calculation results for electron energy states in various small QDs. This parabolic approximation can be used only for large size QDs in the calculation of ground and first excited state energies. The modeling, numerical method, and study presented here not only provide a novel way to calculate the energy levels of QD but also are useful to clarify principal dependencies of QD energy states on material band parameter and QDs size for various QD shapes.

Based on the effective one electronic band Hamiltonian, the energy and position dependent electron effective mass approximation, a finite height hard-wall 3D confinement potential, and the Ben Daniel–Duke boundary conditions, the 3D model has been formulated and solved for the disk, ellipsoid, and conical-shaped InAs/GaAs QDs. To calculate the ground state ($l = 0$) and first excited state ($l = 1$) energy levels, the nonlinear 3D Schrödinger has been solved with a developed nonlinear iterative algorithm to obtain the final self-consistent solutions. In the iteration loops, the Schrödinger equation was discretized with a nonuniform mesh finite difference method, and the corresponding matrix eigenvalue problem was solved with the balanced and shifted QR method. The proposed computational method presented a monotonically convergent property for both the ground and first excited energy states with various QD shapes. The computed results show that for different QD shapes, the parabolic band approximation is applicable only for relatively large dot volume. For the first excited states the non-parabolicity effect also has been found to be stronger than it at ground state.

Acknowledgements

This work was partially supported by the NSC of Taiwan under contract No. NSC89-2215-E-009-055.

References

- [1] D. Bimberg et al., *Thin Solid Films* 367 (2000) 235–249.
- [2] D. Bimberg, *Semicond.* 33 (1999) 951–955.
- [3] N.N. Ledentsov et al., *Semicond.* 32 (1998) 343–365.
- [4] D. Bhattacharyya et al., *IEEE Sel. Top. Quan. Elec.* 5 (1999) 648–657.
- [5] P.A. Maksym et al., *Phys. Rev. Lett.* 65 (1990) 108–111.
- [6] R. Leon et al., *Phys. Rev. B* 58 (1998) R4262–R4265.
- [7] F. Heinrichsdorff et al., *J. Crystal Growth* 195 (1998) 540–545.
- [8] M. Perret et al., *Phys. Rev. B* 62 (2000) 5092–5099.
- [9] X.Z. Liao et al., *Phys. Rev. B* 58 (1998) R4235–R4237.
- [10] H. Gotoh et al., *Appl. Phys. Lett.* 72 (1998) 1341–1343.
- [11] Z.R. Wasilewski et al., *J. Crystal Growth* 201/202 (1999) 1131–1135.
- [12] I. Mukhametzanov et al., *Appl. Phys. Lett.* 75 (1999) 85–87.
- [13] H. Saito et al., *Appl. Phys. Lett.* 74 (1999) 1224–1226.
- [14] J.P. McCaffrey et al., *J. Appl. Phys.* 88 (2000) 2272–2277.
- [15] P.W. Fry et al., *Physica E* 9 (2001) 106–113.
- [16] G. Lamouche et al., *Phys. Rev. B* 51 (1995) 1950–1953.
- [17] F.M. Peeters et al., *Phys. Rev. B* 53 (1996) 1468–1474.
- [18] A. Wojs et al., *Phys. Rev. B* 54 (1996) 5604–5608.
- [19] A.H. Rodríguez et al., *Phys. Rev. B* 63 (2001) 125 319–125 327.
- [20] P. Lelong et al., *Solid State Comm.* 98 (1996) 819–823.
- [21] D.M.T. Kuo et al., *Phys. Rev. B* 61 (2000) 11 051–11 056.
- [22] N. Singh et al., *Int. J. Mod. Phys.* 14 (2000) 1753–1766.
- [23] M. Grudman et al., *Phys. Rev. B* 52 (1995) 11 969–11 981.
- [24] O. Stier et al., *Phys. Rev. B* 59 (1999) 5688–5701.
- [25] M. Califano et al., *Phys. Rev. B* 61 (2000) 10 959–10 965.
- [26] M. Califano et al., *J. Appl. Phys.* 88 (2000) 5870–5874.
- [27] J. Shumway et al., *Physica E* 8 (2000) 260–268.
- [28] S.S. Li et al., *J. Appl. Phys.* 84 (1998) 3710–3713.
- [29] P.C. Sercel et al., *Phys. Rev. Lett.* 83 (1999) 2394–2397.
- [30] H. Jiang et al., *Phys. Rev. B* 56 (1997) 4696–4701.
- [31] C. Pryor, *Phys. Rev. B* 60 (1999) 2869–2874.
- [32] S. Bednarek et al., *Phys. Rev. B* 59 (1999) 12 042–13 036.
- [33] L.R.C. Fonseca et al., *Phys. Rev. B* 57 (1998) 4017–4026.
- [34] R.S. Varga, *Matrix Iterative Analysis*, Prentice-Hall, 2000.
- [35] D.S. Watkins, *J. Comp. App. Math.* (2000) 67–83.
- [36] J.H. Wilkinson, C. Reinsch, *Linear Algebra II of Handbook for Automatic Computation*, Springer-Verlag, 1971.
- [37] I.C.F. Ipsen, *SIAM Rev.* 39 (1997) 254–291.
- [38] G. Bastard, *Wave Mechanics Applied to Semiconductor Heterostructures*, Les Edition de Physique, Halsted Press, New York, 1988.
- [39] S.L. Chuang, *Physics of Optoelectronic Devices*, John Wiley & Sons, New York, 1995.
- [40] G.H. Golub et al., *Matrix Computations*, The Johns Hopkins University Press, 1996.
- [41] M. Levinshstein et al., *Handbook Series on Semiconductor Parameters*, World Scientific, Singapore, 1999.